ACS OMEGA

Article

http://pubs.acs.org/journal/acsodf

Compound Ranking Based on Fuzzy Three-Dimensional Similarity Improves the Performance of Docking into Homology Models of G-Protein-Coupled Receptors

Andrew Anighoro and Jürgen Bajorath*

Department of Life Science Informatics, B-IT, LIMES Program Unit Chemical Biology and Medicinal Chemistry, Rheinische Friedrich-Wilhelms-Universität, Dahlmannstr. 2, D-53113 Bonn, Germany

ABSTRACT: Ligand docking into homology models of G-protein-coupled receptors (GPCRs) is a widely used approach in computational compound screening. The generation of "double-hypothetical" models of ligand−target complexes has intrinsic accuracy limitations that further complicate compound ranking and selection compared to those of X-ray structures. Given these uncertainties, we have explored "fuzzy 3D similarity" between hypothetical binding modes of known ligands in homology models and docking poses of database compounds as an alternative to conventional scoring schemes. Therefore, GPCR homology models at varying accuracy levels were generated and used for docking. Increases in recall performance were observed for fuzzy 3D similarity ranking using single or multiple ligand poses compared to that of conventional scoring functions and interaction fingerprints. Fuzzy similarity ranking was also successfully applied to docking into an external model of a GPCR for which no experimental structure is currently available. Taken together, our results indicate that the use of putative ligand poses, albeit approximate at best, increases the odds of identifying active compounds in docking screens of GPCR homology models.

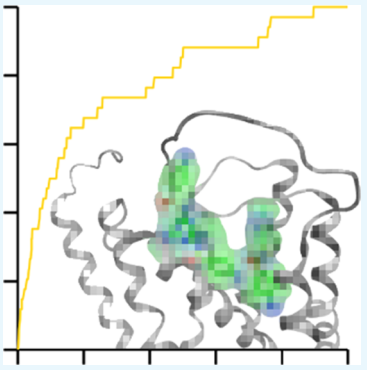

1. INTRODUCTION

Docking of small molecules into binding sites of target proteins continues to be the major approach to computational ligand identification.[1,2] Although high-resolution X-ray structures are generally preferred as docking templates, homology models are also frequently used in the absence of experimental structures.[3−5] Although protein models are less accurate than X-ray structures from which they are derived, they are also capable of enriching active compounds in database rankings from docking screens and identifying new active compounds in prospective applications.[6]

G-protein-coupled receptors (GPCRs) are a growth area for molecular docking, due to stellar advances in the structural biology of these highly complex membrane receptor systems over the past decade.[7−9] The increasing number of experimentally determined GPCR structures has deepened our understanding of binding-site features and provided unprecedented opportunities for structure-based compound screening and ligand design.[10] At the same time, structural coverage across the GPCR superfamily is still sparse compared to that of other popular therapeutic targets. Accordingly, homology models of GPCRs continue to play an important role for docking,[11,12] yielding impressive results in some applications.[6] In fact, with each new GPCR X-ray structure that is becoming available, the knowledge base for homology modeling further increases compared to that of earlier days when the X-ray structure of bovine rhodopsin was for long the only available template for GPCR modeling.[13,14]

Despite incremental advances made over the years, force field-based scoring of ligand poses still represents a major limitation of hit identification via docking.[15−17] Difficulties in reliably ranking active compounds on the basis of force field energy functions have triggered the exploration of alternative scoring approaches tailored toward different targets or families, including GPCRs.[18−20] In this context, synergies between docking and ligand-based computational screening methods can also be taken into consideration,[21,22] for example, the inclusion of molecular similarity[23] in evaluating docking poses. However, only few studies have so far attempted to combine ligand-based similarity assessment and docking, for example, through sequential calculations[24,25] or data fusion.[26]

As a step toward integration of molecular similarity and docking calculations, we have previously reported a methodology combining the generation of docking poses with 3D similarity comparison to experimentally determined ligand-binding modes.[27] Accordingly, instead of applying scoring functions, docking poses and reference ligands were compared and 3D similarity values calculated to generate database rankings, which frequently yielded significant improvements in compound recall over conventional scoring or the use of protein−ligand interaction fingerprints (PLIFs) for pose prioritization.[27,28] In addition to other targets, the utility of this approach was also demonstrated for GPCRs.[28] However, given the dependence of the 3D similarity-based approach on crystallographic ligand

Received: March 20, 2017
Accepted: May 31, 2017
Published: June 8, 2017

DOI: 10.1021/acsomega.7b00330
ACS Omega 2017, 2, 2583−2592

binding modes, its application was principally limited to targets for which complex X-ray structures were available.

Herein, we explored 3D similarity-based compound ranking for docking into homology models of GPCRs, which continue to be widely used in virtual screening. This might appear to be counterintuitive at a first glance because 3D similarity ranking was conceptually based on crystallographic ligand-binding modes. The probability to correctly prioritize docking poses was expected to increase with the increase in the accuracy of the reference information. However, given that docking into homology models yields "double-hypothetical" ligand−target complexes[29] with principally limited accuracy, we were interested in investigating whether "fuzzy similarity" between the modeled reference and database compounds might also suffice to guide compound selection. Therefore, different strategies were evaluated for ranking on the basis of fuzzy similarity, including single or multiple reference poses. As reported herein, these strategies produced higher compound recall for GPCR homology models than force field energy scoring or PLIFs, thus further extending the potential of model-based compound selection.

2. METHODS AND MATERIALS

2.1. Receptor Structures and New Homology Models. An X-ray structure of the β_2 adrenergic (β_2) receptor bound to the antagonist carazolol (PDB code 2RH1[30]) was taken from the Protein Data Bank. The structure was prepared for docking using Molecular Operating Environment (MOE) 2014.09.[31] Bound ions, organic solvent, and water molecules were removed from the receptor ligand-binding domain used as a template for docking. Other preparation steps included the addition of hydrogen atoms, computation of protonation states and tautomers (calculated at pH 7), assignment of partial charges, and limited energy minimization (structural relaxation) using the Amber10 force field until a root mean square (RMS) gradient of 0.1 kcal/mol/Å^2 was reached.

Two homology models of the β_2 receptor were built using the structure of β_1 adrenergic (β_1) receptor (PDB code 4BVN)[32] from turkey (*Meleagris gallopavo*) and human adenosine A_{2A} (A_{2A}) receptor (PDB code 4EIY)[33] as templates, respectively. In addition, a homology model of the A_{2A} receptor was generated using the β_2 receptor, 2RH1, as a template. The modeling protocol detailed in the following was consistently applied.

Initial sequence alignments were generated with Clustal Omega.[34] For homology modeling, the alignments were manually edited to appropriately place insertions and deletions in variable regions. In each case, MODELLER version 9.17[35] was used to build 500 initial models, and the one with the most favorable DOPE energy score was selected. Selected models were prepared for docking as described above for the X-ray structure. A known antagonist was flexibly docked into the binding site of each selected model to refine binding site coordinates and provide a reference binding mode. Ligands included ZM241385[33] (for A_{2A}) and carazolol[30] (for β_2). To adjust side chain positions of the residues in the modeled binding sites in a ligand-assisted manner, the induced-fit docking protocol of MOE[31] was applied, permitting side chain flexibility within 6 Å of the placed ligand. In each case, 100 of 100 000 initially generated docking poses were retained and scored with the GBVI/WSA dG function implemented in MOE using default parameter settings. As a reference for RMSD calculations, crystallographic binding modes of reference ligands were transferred into the models following α carbon atom superposition of the X-ray structures and corresponding models.

2.2. External GPCR Model. A homology model of the 5-hydroxytryptamine 6 (5-HT_6) receptor was extracted from the GPCRdb.[36] This database includes various models of human GPCRs generated by fragment assembly from different templates for backbone construction combined with position-specific rotamer side chain modeling.[37] The 5-HT_6 receptor model was prepared for docking as described above.

2.3. Compound Sets. A benchmark set for the A_{2A} receptor was extracted from the DEKOIS 2.0.[38] The selected data set included 37 antagonists and 1100 corresponding decoys. To focus the study on the ranking of antagonists, the only three known agonists (BDB50085666, BDB50085668, and BDB50309479) present in the benchmark set were removed together with 100 decoys selected by the developers of the DEKOIS database to match physicochemical properties of these agonists. Activity annotations were confirmed on the basis of the corresponding BindingDB[39] records. For β_2, no functional designation (agonist or antagonist) was provided for a number of ligands in DEKOIS. Therefore, 23 known antagonists were taken from the IUPHAR/BPS Guide to Pharmacology database (GtoPdb).[40] These compounds were found to correspond to 15 different Bemis−Murcko (BM) scaffolds, indicating structural diversity. For these antagonists, 1150 decoys were generated via the DUD-E web server.[41] For the external GPCR model, a set of 35 5-HT_6 antagonists (containing 32 unique BM scaffolds) was extracted from GtoPdb[40] and 2350 decoys were generated using DUD-E.[41]

For each compound, an initial low-energy conformation was generated with MOE and protonation states and partial charges were assigned on the basis of its AM1-BCC implementation following a previously reported protocol,[42] which was also applied to prepare crystallographic ligands for docking.

2.4. Docking and Scoring. All docking trials were carried out using the Dock module of MOE.[31] The triangle matcher function was used to generate 1000 docking poses for each ligand, and the top 30 poses on the basis of the London dG scoring function were preselected and further refined by rescoring using the GBVI/WSA dG scoring function to produce final ranking. In previous studies,[27,28] this combination of the London dG and GBVI/WSA dG functions was the consistently best performing force field-based scoring scheme.

2.5. Similarity Calculations. Similarity to reference binding modes was quantified using a property density function-based 3D similarity measure[43] that was consistently applied in our previous studies for 3D similarity evaluation of docking poses.[27,28] In addition, interaction similarity was assessed on the basis of the PLIF implementation of MOE.[31] In the former case, normalized overlap of property density functions (ranging from 0 to 1) was calculated as a measure of 3D similarity.[43] Accordingly, both conformational and translational differences (e.g., different orientations in a binding site and/or positional displacements) were taken into account. In the latter case, receptor−ligand contacts were assigned to six categories of interactions including side chain-mediated hydrogen bonds (donor and acceptor), backbone-mediated hydrogen bonds (donor and acceptor), ionic interactions, and surface interactions. PLIFs were calculated with default settings and compared using the Tanimoto coefficient.[44] For each similarity measure, compound rankings were calculated.

The reference ligands used for similarity calculations were overall characterized by relatively low similarity to the docked

DOI: 10.1021/acsomega.7b00330
ACS Omega 2017, 2, 2583−2592

antagonists. Only one to two antagonists in each data set had a two-dimensional (2D) similarity value of greater than 0.8 calculated using MACCS fingerprint compared to that of the reference compounds.

2.6. Performance Evaluation. Receiver operator characteristic (ROC) plots were generated to evaluate compound rankings. ROC curves monitor the percentage of known active compounds retrieved at each position of the ranking. The area under the ROC curve (AUC) was calculated as a measure of the enrichment of active compounds in a ranking applying the composite trapezoidal rule. AUC values of 0.5 correspond to the random distribution of active compounds and decoys in rankings, whereas increasing AUC values greater than 0.5 further indicate increasing enrichment of active compounds at high-rank positions. Accordingly, an AUC value of 1 would be produced by a ranking in which all active compounds would be ranked higher than the best scoring decoys. In addition, to specifically assess early enrichment of active compounds, the enrichment factor for 10% of the ranked database (E_f10%) was also computed.[45] The maximum theoretical E_f10% for all three data sets was 10.

For the external homology model, the performance was also assessed by calculating E_f1% values. The maximum theoretical E_f1% for this data set was 68.6. Furthermore, Rocker[46] was used to calculate BEDROC[47] values with α = 20.0.

3. RESULTS AND DISCUSSION

3.1. Study Concept. Previously, we have ranked docking poses on the basis of 3D similarity to crystallographic ligand-binding modes as an alternative to conventional force field scoring.[27,28] These were the first attempts to calculate 3D similarity for compound ranking from docking screens, which represents, by definition, a knowledge-based approach. The ability of 3D similarity calculations to enrich active compounds at high-rank positions was attributed to the use of well-defined experimental ligand-binding modes as references that many active compounds were anticipated to resemble. In fact, core fragments of crystallographic ligands were in some instances already sufficient to effectively guide compound ranking.[28] Herein, we have investigated the question whether approximate ligand poses might also be useful. For example, in cases in which no complex structures are available, known active compounds might be docked into X-ray structures of targets to provide reference poses. If modeled poses would at least be approximately correct, they might serve as a surrogate or alternative for scoring. We also reasoned that the use of approximate ligand-binding modes might be particularly suitable if the docking template itself was approximate, that is, a computational model instead of a refined X-ray structure. Hence, we essentially asked the question whether the odds of docking into approximate models might be further improved by adding one or more hypothetical compound-binding modes as a basis for compound ranking. However, propagating inaccuracies resulting from modeling of targets and complexes might also compromise similarity-based ranking. In any event, the use of double-hypothetical models inevitable introduces fuzziness into 3D similarity assessment, which is not due to the similarity calculations (which are the same as for crystallographic references) but rather to the use of approximate reference states. Fuzziness of these calculations might be further increased by using alternative binding poses instead of a single one. Because the assessment of fuzzy similarity for compound ranking was the main motivation for our current study, the analysis was deliberately focused on homology models of GPCRs, which continue to be popular docking targets. Owing to advances in GPCR crystallography, homology modeling of GPCRs has experienced a renaissance in recent years.

3.2. Docking into the X-ray Structure of the β_2 Receptor. As a reference calculation, 3D similarity scoring was initially applied to the X-ray structure of the β_2 receptor complexed to the antagonist carazolol. Three alternative rankings were generated on the basis of 3D similarity to the bound antagonist carazolol, PLIF-based similarity, and the preferred scoring function. The results are summarized in Table 1 and graphically represented in Figure 1A. Both scoring and 3D similarity calculations resulted in a high enrichment of known antagonists with an AUC of 0.80 and 0.83, respectively, and an E_f10% of 6.09 for both methods. By contrast, PLIF-based similarity only resulted in an AUC of 0.62. Figure 2 shows that PLIF-based ranking was very sensitive to correct posing. When docked antagonists departed from the binding of carazolol, even if only in part, ligand−receptor interaction details were modulated, thereby reducing PLIF similarity and leading to low ranks. In contrast, 3D similarity calculations were much more robust and yielded comparably high ranks for antagonists as long as the docking poses were at least approximate and parts of ligands correctly aligned. Importantly, 3D similarity calculations quantify whole-molecule resemblance by comparing atomic property density functions but are insensitive to interaction differences, which provided an advantage in this case. For the A_{2A} receptor in which ligand−receptor key interactions were mainly formed by a large rigid aromatic ring system, posing was more stable than observed for the β_2 receptor herein and central interactions often conserved, leading to more successful PLIF-based ranking of known antagonists A_{2A}.[28] In the presence of approximate poses, 3D similarity assessment was clearly more effective.

Table 1. Docking Screen of the β_2 Receptor Structure[a]

protocol	reference pose	AUC	E_f10%
FF scoring	none	0.80	**6.09**
3D similarity	X-ray	**0.83**	**6.09**
PLIF similarity	X-ray	0.62	4.35

[a]Compounds were docked into the β_2 receptor structure (PDB code 2RH1) and ranked on the basis of force field (FF) energy scoring and 3D similarity as well as the PLIF similarity to the X-ray structure of a bound ligand. Recall of active compounds is reported. Results for the best performing methods are in bold.

3.3. Docking into Homology Models. For the next step, three homology models were built, including two of the β_2 and one of the A_{2A} receptor (Table 2). The two β_2 models were constructed to represent different accuracy levels. The first model was built using the structure of the β_1 adrenergic (β_1) receptor from turkey as a template. This model is referred to as $\beta_2(\beta_1)$. The β_1 template and β_2 receptors shared high sequence identity and conserved binding site residues, yielding an overall accurate model (RMSD 1.72 Å; magenta in Figure 3A). The alternative model was obtained using the structure of the human A_{2A} receptor as a template, referred to as $\beta_2(A_{2A})$. Although β_1, β_2, and A_{2A} belonged to class A (rhodopsin-like) GPCRs, β_2 shared much lower sequence identity with A_{2A} than with β_1 (Table 2). The $\beta_2(A_{2A})$ model was thus overall less accurate (RMSD of 3.06 Å; orange in Figure 3A), including the ligand binding that was only partly conserved in β_1 and A_{2A} (Figure 3B). In addition, an approximate homology model of the A_{2A} receptor

DOI: 10.1021/acsomega.7b00330
ACS Omega 2017, 2, 2583−2592

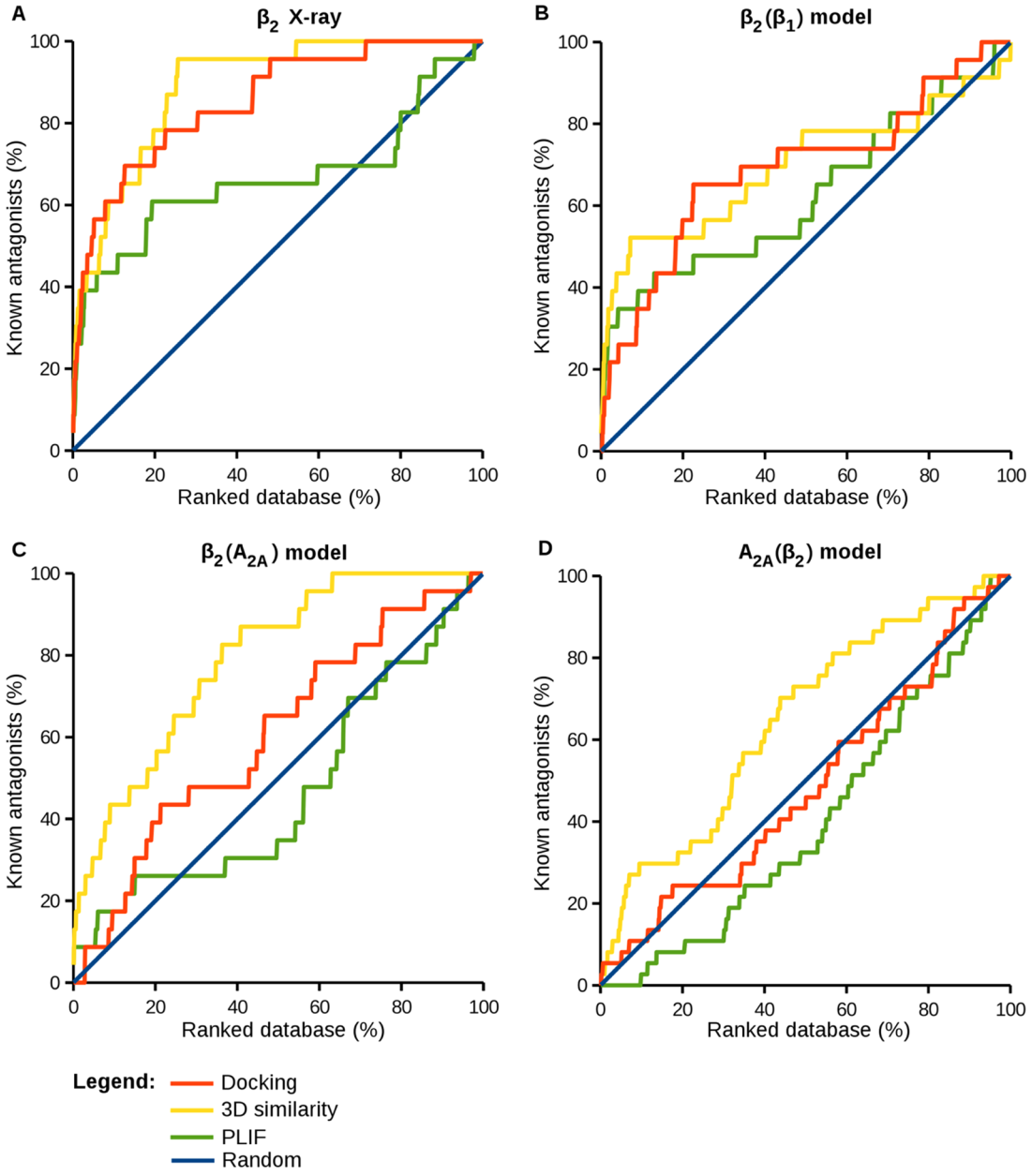

Figure 1. ROC plots for alternative ranking schemes. Orange curves represent the results for the London dG scoring function and yellow curves for 3D similarity to the crystallographic binding mode of carazolol (panel A), a docking pose of carazolol (panels B and C), or a docking pose of a fragment of ZM241385 (consisting of the triazolotriazine core and the furan ring) (panel D). Green curves represent the results for PLIF-based compound ranking by using the same reference poses as before, and the blue lines provide a reference for random compound selection.

was also generated using the β_2 receptor as a template, referred to as $A_{2A}(\beta_2)$ (RMSD 3.62 Å; pink in Figure 3C). Overall, $A_{2A}(\beta_2)$ was the least accurate homology model, and binding site accuracy of this model was also only limited (Figure 3D), as expected.

Induced-fit docking was used to generate reference binding modes of carazolol for the β_2 models and of ZM241385 for the A_{2A} models. For β_2, the accuracy of the modeled binding modes of carazolol correlated with the accuracy of the models. Thus, in $\beta_2(\beta_1)$, the pose was close to the experimental binding mode (RSMD 1.2 Å; magenta in Figure 3B), whereas the pose was displaced in $\beta_2(A_{2A})$ with only partial structural overlap (RMSD 5.7 Å; orange in Figure 3B). For ZM241385A, a pose was obtained that also displayed a partial displacement but was overall well aligned with the experimental binding mode (RMSD 1.8 Å; Figure 3D). In the case of $\beta_2(\beta_1)$ and $\beta_2(A_{2A})$, the pose with the lowest RMSD value generated by the induced-fit docking protocol did not correspond to the one with the best score that was selected as a reference. A pose with an RMSD value of 0.5 Å was obtained for $\beta_2(\beta_1)$ and another with an RMSD of 3.5 Å for $\beta_2(A_{2A})$. For consistency with our validation study, these poses were not selected as a reference.

For the three homology models, docking screens were carried out using specifically assembled sets of antagonists and decoys. For $\beta_2(\beta_1)$ and $\beta_2(A_{2A})$, AUC values of 0.69 and 0.61 were obtained, respectively (Table 3), whereas for $A_{2A}(\beta_2)$, the least accurate model, the recall of known antagonists on the basis of scoring, was close to a random selection (Table 3). Hence, compound recall for homology models was lower than for the corresponding X-ray structure and dependent on the accuracy of the models, consistent with our expectation.

DOI: 10.1021/acsomega.7b00330
ACS Omega 2017, 2, 2583−2592

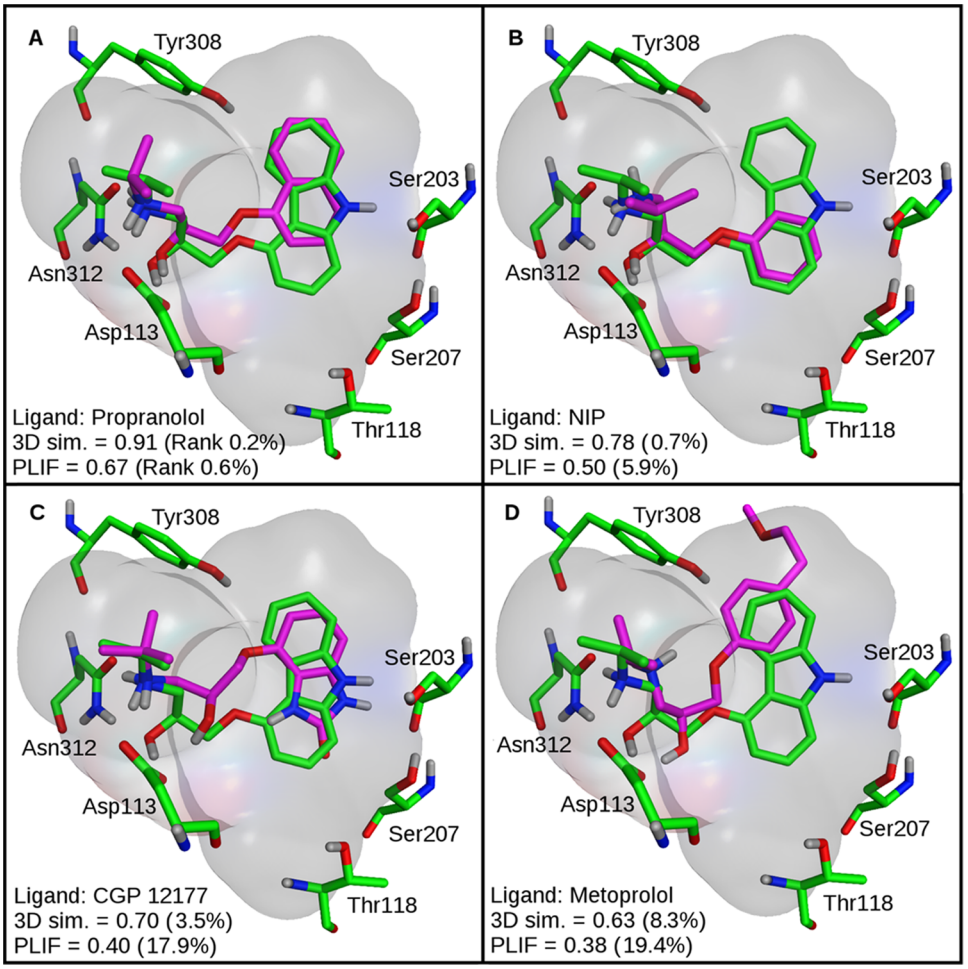

Figure 2. 3D similarity vs PLIFs. Superposition of co-crystallized carazolol (green) and four representative docked antagonists (magenta) are shown. In panel A, propranolol essentially matches all structural features of carazolol and hence forms comparable interactions with the receptor. In panel B, NIP also aligns well with carazolol, but the protonated amine is too far away from Asp113 for forming a salt bridge. In panel C, a salt bridge between CGP 12177 and Asp113 is present, but the hydroxyl group is displaced and the aromatic ring system is found in a head-to-tail orientation compared to that of carazolol. In panel D, metoprolol only partly overlaps with carazolol and does not form well-defined interactions. For each antagonist, 3D similarity scores and percentage rank positions (in parentheses) are reported.

Table 2. In-House Homology Models[a]

model	template	sequence identity (%)	template PDB code	template resol. (Å)	model RMSD (Å)	pocket RMSD (Å)	docked ligand RMSD (Å)	DOPE score
β_2	β_1	52.9	4BVN	2.1	1.7	0.5	1.2	−41 854.8
β_2	A_{2A}	30.4	4EIY	1.8	3.1	2.3	5.7	−39 094.1
A_{2A}	β_2	30.4	2RH1	2.4	3.6	3.6	1.8	−38 530.9

[a]For two GPCRs with known X-ray structures, homology models were generated using different templates. All template structures were from *Homo sapiens*, except β_1, which was from *M. gallopavo*. For templates and targets, sequence identity is reported. For template structures, the crystallographic resolution is also given. In addition, RMSD values are provided for comparison of each model with the corresponding X-ray structure, residues forming the binding pocket, and docked ligands and their crystallographic binding modes (after superposition of the model and X-ray structure). DOPE scores computed by MODELLER to assess model quality are also reported.

Next, docking trials were carried out using the induced-fit docking poses of carazolol and ZM241385 described above as reference binding modes. In the case of ZM241385, only the core fragment composed by the triazolotriazine core and furan ring was considered, which dominated the 3D similarity calculations on X-ray templates.[28] For all three models, an increase in compound recall and early enrichment was observed for 3D similarity ranking compared to that of scoring, as reported in Figure 1B–D and Table 3.

For the $\beta_2(\beta_1)$ and $\beta_2(A_{2A})$ models, the use of induced-fit docking poses as a reference for 3D similarity calculations resulted in AUC values of 0.70 and 0.79, respectively, and even for $A_{2A}(\beta_2)$ a value of 0.65, although scoring was in this case not better than random selection. By contrast, PLIF scoring only produced an enrichment for $\beta_2(\beta_1)$, with an AUC value of 0.63, but was below random selection in the other cases, which further illustrated the difficulties to score approximate interactions; a ranking strategy we consider unsuitable for models. In contrast, 3D similarity calculations were successful. Even ligands displaced

DOI: 10.1021/acsomega.7b00330
ACS Omega 2017, 2, 2583−2592

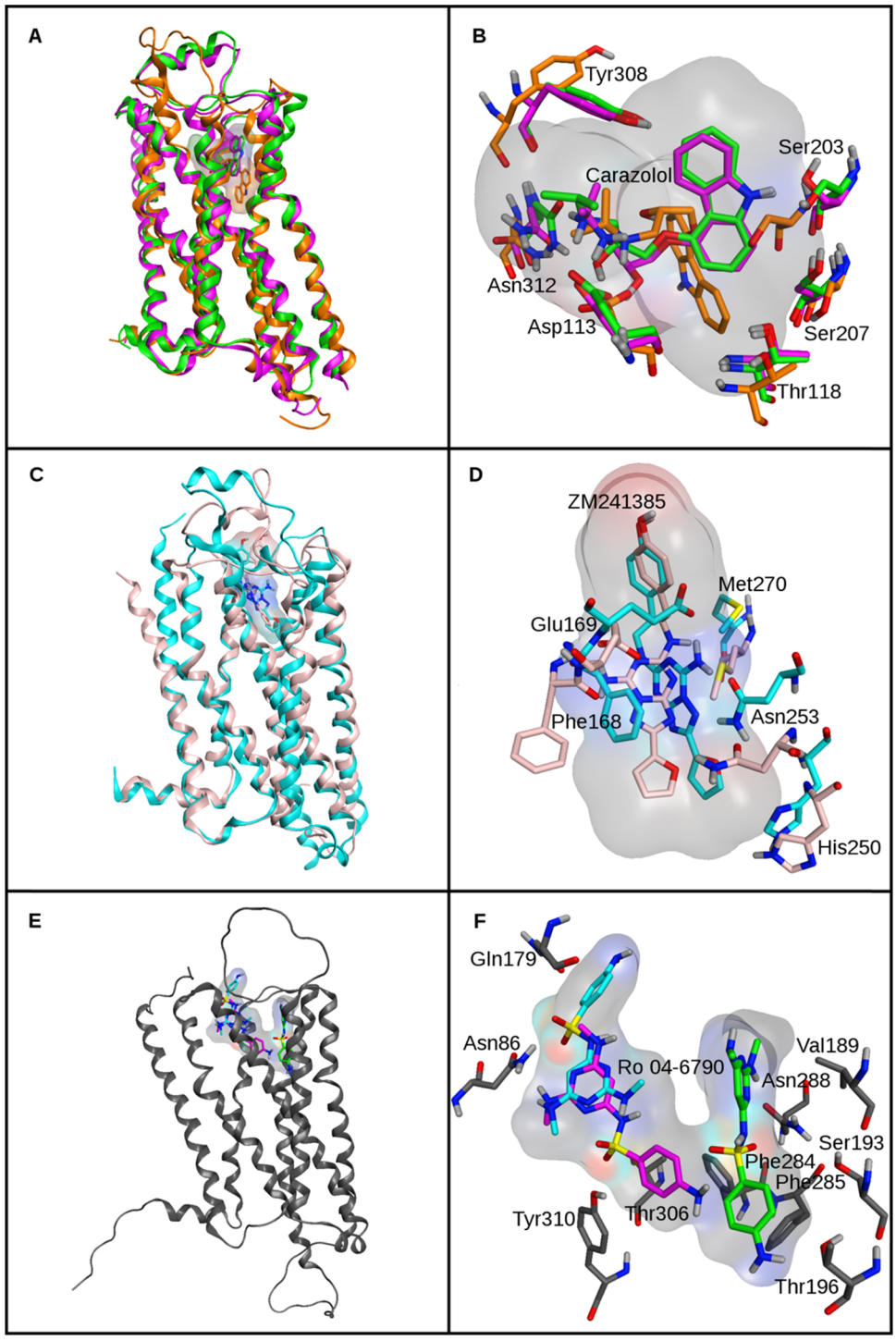

Figure 3. Structures and binding modes. Panel A shows the superposition of the X-ray structure of the β_2 receptor (green) and two homology models based on the β_1 (magenta) and the A_{2A} (orange) receptor, respectively. In panel B, binding site details are displayed including co-crystallized carazolol (green) and modeled binding modes. Panel C shows the superposition of the X-ray structure of the A_{2A} receptor (cyan) and the β_2 receptor-based model (pink). In panel D, binding site details are shown including co-crystallized ZM241385 (cyan) and modeled binding modes. Panel E shows the homology model of the 5-HT_6 receptor from GPCRdb. In panel F, binding site details are displayed including three different docking poses of Ro 04-6790.

in homology models relative to their crystallographic binding modes, as shown in Figure 2, were sufficient to guide compound selection on the basis of 3D similarity and achieve better enrichment than energy scoring. Thus, as long as the orientation of a reference ligand within the binding site was at least approximately correct, 3D similarity calculations were robust and tolerant to limited inaccuracies when using homology models and hypothetical complexes.

3.4. Multiple Reference Poses. In light of the positive results obtained for individual ligand poses, we also asked the question whether the use of multiple poses might further improve compound ranking. Taking inherent accuracy limitations into account, multiple poses further increase the degree of

DOI: 10.1021/acsomega.7b00330
ACS Omega 2017, 2, 2583−2592

Table 3. Docking Screens of In-House Homology Models[a]

protocol	reference pose	AUC $\beta_2(\beta_1)$	AUC $\beta_2(A_{2A})$	AUC $A_{2A}(\beta_2)$	E_f10% $\beta_2(\beta_1)$	E_f10% $\beta_2(A_{2A})$	E_f10% $A_{2A}(\beta_2)$
FF scoring	none	0.69	0.61	0.49	3.48	1.74	1.08
3D similarity	Ind. Fit	0.70	**0.79**	0.65	5.22	**4.35**	2.97
	Top 3 S.	0.69	**0.79**	0.50	5.00	4.09	0.83
	Top 3 Dif.	**0.82**	0.76	**0.76**	**5.45**	3.18	**4.72**
PLIF similarity	Ind. Fit	0.63	0.47	0.40	3.92	1.74	0.27
	Top 3 S.	0.60	0.43	0.52	3.18	1.36	1.94
	Top 3 Dif.	0.62	0.50	0.53	1.82	2.73	1.67

[a]Reported is the recall performance for docking into different homology models using alternative ranking schemes. For 3D and PLIF similarity, three different reference pose schemes are evaluated. "Ind. Fit" stands for induced fit, "Top 3 S." refers to the three top-scoring ligand docking poses, and "Top 3 Dif." to three dissimilar docking poses. Results for the best performing methods are in bold.

fuzziness underlying similarity calculations. If multiple poses were used, it would be possible to select for each docked compound the pose yielding the highest 3D similarity values and use this value for compound ranking. This scenario corresponded to a nearest-neighbor (1-NN) search in the pose space. Accordingly, it might be possible to balance inaccuracies associated with single putative binding modes.

To test this hypothesis, preferred binding modes were collected for the reference ligands carazolol and ZM241385 using rigid receptor docking into the models and two alternative sets of three poses each were assembled as references for 1-NN calculations. The first set consisted of the three best-scoring binding modes (Top 3 S.), regardless of their structural relationships, and the second set consisted of the three poses with the largest RMSD values among the precomputed binding modes (Top 3 Dif.) The idea underlying the generation of the second set was further increasing binding site coverage with poses for 1-NN calculations.

Ranking by 3D similarity to these pose sets produced different results. Whereas the use of the Top 3 S. sets did not lead to a further improvement in compound ranking compared to that of the individual ligand-binding modes, the use of Top 3 Dif. sets resulted in a notable improvement for $\beta_2(\beta_1)$ and $A_{2A}(\beta_2)$, as reported in Figure 1A–C and Table 3. For $\beta_2(A_{2A})$, recall performance remained essentially constant when using single or multiple ligand poses. For $\beta_2(\beta_1)$ and $A_{2A}(\beta_2)$, large AUC values of 0.82 and 0.76 were obtained, respectively, together with large early enrichment factors (5.45 and 4.72, respectively). Hence, overall, the use of Top 3 Dif. pose sets was the preferred strategy for compound ranking.

These results suggest that an enhanced conformational sampling of reference poses may be beneficial for compound ranking. A potential extension of this approach may include the generation of reference poses via molecular dynamics or Monte Carlo simulations. This would also enable sampling different conformations of both the ligand and the receptor, thus partly accounting for protein flexibility.

3.5. Docking Screen of an External Model. To further assess the use of multiple ligand-binding modes for compound ranking, we also applied the preferred Top 3 Dif. strategy to an externally derived homology model of a GPCR. For this purpose, a model of the 5-HT_6 receptor was selected (Figure 3E), another topical drug target.[48,49] Structures of two other subtypes of the 5-HT receptor, including 5-HT_{1B} and 5-HT_{2B}, were reported in complex with agonists,[50,51] but the structure of 5-HT_6 is currently unknown. In addition, compared with our in-house homology models, the 5-HT_6 model was generated from multiple templates using a different computational protocol.[37] Given the absence of an X-ray structure, the accuracy of this model remained unknown.

For 5-HT_6, a set of 35 antagonists and 2350 decoys was assembled and used for docking into the putative binding pocket of the model. Reference binding modes were obtained by generating Top 3 Dif. docking poses of the known antagonist, Ro 04-6790 (Figure 3F), one of the first 5-HT_6 selective antagonists that was discovered.[52] Three-dimensional similarity-based ranking resulted in an AUC of 0.75 and E_f10% of 3.53 (Table 4). As a control, force field-based scoring performed surprisingly well for this model (in fact, better than that observed for the other GPCR models), with an AUC of 0.77 and E_f10% of 3.14, hence yielding overall comparable results (Table 4). This trend was reflected by the equivalent BEDROC values measured for the two approaches (Table 4). Nonetheless, 3D similarity calculations resulted in higher enrichment of known antagonists within the first third of the ranking (Figure 4D).

Table 4. Docking Screen of the External Homology Model of the 5-HT_6 Receptor[a]

protocol	reference pose	AUC	E_f1%	E_f10%	BEDROC
FF scoring	none	**0.77**	5.71	3.14	**0.22**
3D similarity	Top 3 Dif.	0.75	**5.88**	**3.53**	**0.22**

[a]Recall performance is compared for docking into the homology model of the 5-HT_6 receptor on the basis of best force field energy scoring and the preferred "Top 3 Dif." 3D similarity pose strategy. E_f1% and BEDROC (α = 20.0) are reported as an additional performance assessment. Results for the best performing methods are in bold.

3.6. Control Calculations. As additional control calculations, each of the 23 antagonists in the β_2 data set was docked into the β_2 X-ray structure and homology models and used as a reference for single-pose 3D similarity calculations. A consistent enrichment of active compounds was observed, with average AUC values over all of the 23 trials ranging from 0.60 for $\beta_2(\beta_1)$ to 0.78 for β_2 X-ray structure. Thus, these calculations demonstrated that 3D similarity calculations did not depend on individual antagonists used as references. However, inverting the orientations of reference binding modes within the binding site in a "head-to-tail" manner by 180° mostly abolished the enrichment of active compounds, demonstrating that at least approximately correct ligand orientations were essential for fuzzy 3D similarity calculations.

A correlation analysis was carried out between the 3D similarity measured for all of the compounds docked into the β_2 X-ray structure by taking the crystallographic binding mode of

DOI: 10.1021/acsomega.7b00330
ACS Omega 2017, 2, 2583–2592

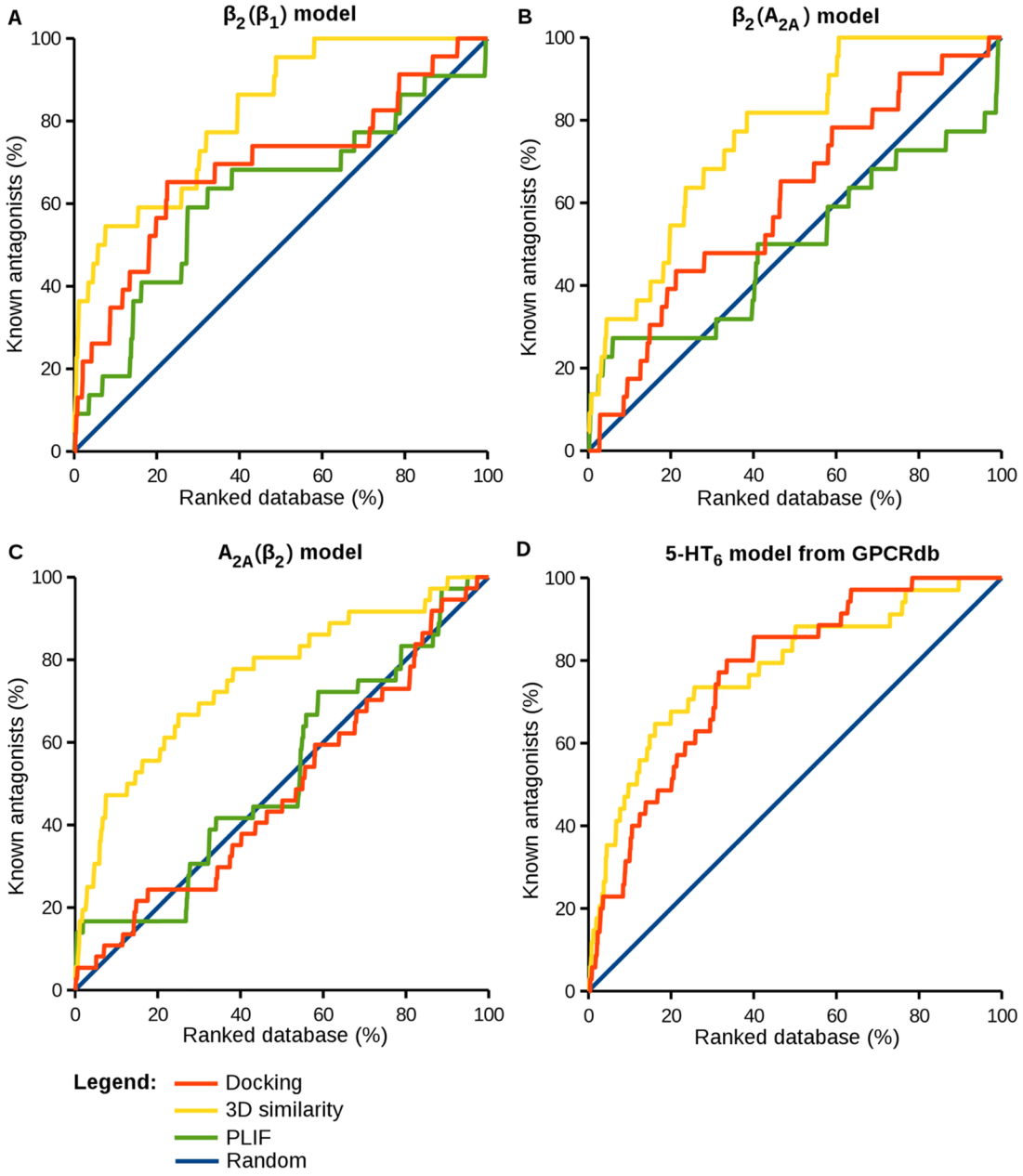

Figure 4. ROC plots for ranking based on similarity to three different docking poses. Yellow curves represent the results for compound ranking on the basis of 3D similarity calculations relative to three different docking poses of carazolol (panels A and B), a fragment of ZM241385 (consisting of the triazolotriazine core and the furan ring; panel C), or Ro 04-6790 (panel D). For comparison, green curves represent the results for PLIF-based compound ranking by using the same reference poses as before and orange curves the results for the London dG scoring function. The blue lines provide a reference for random compound selection.

carazolol as reference and 2D similarity to the same ligand on the basis of ECFP4 fingerprints. A low correlation coefficient (r = 0.29) was obtained. This finding was consistent with previous studies, indicating frequent low correlation of 3D and 2D ligand similarities.[27,43]

4. CONCLUSIONS

Scoring and compound ranking continue to be limiting factors of docking screens. While docking algorithms have become increasingly effective over the years, it continues to be difficult to separate active from inactive compounds in rankings. As a consequence, potential alternatives to force field energy scoring are considered. Among these is the calculation of 3D similarity of test compounds relative to binding modes of known ligands, for which proof-of-principle has been established previously. Although this approach has been firmly rooted in X-ray crystallography to provide reference binding modes, we have investigated herein whether it might be further extendable to docking tasks wherein accuracy is principally limited, that is, when homology models are used as docking templates. Despite accuracy limitations, the use of homology models is relevant for the practice of structure-based virtual screening, especially when GPCRs are targeted. Perhaps provocatively, we have asked the question whether putative reference binding modes placed into homology models might be useful to guide compound ranking and designed a study to investigate this question in detail. Therefore, the approach reported herein deliberately introduced fuzziness into 3D similarity assessment at the level of modeled

DOI: 10.1021/acsomega.7b00330
ACS Omega 2017, 2, 2583−2592

binding modes. Success or failure of such calculations was essentially unpredictable. However, for different GPCR models, our analysis revealed that fuzzy 3D similarity calculations were indeed capable of further enriching active compounds at high-ranking positions compared to that of other scoring schemes, as long as modeled binding modes and orientations were at least approximately correct. Moreover, ensembles of multiple structurally diverse poses in combination with the nearest-neighbor similarity calculations were overall more effective in compound ranking than single binding modes, which further increased the fuzziness of the approach. Taken together, the findings reported herein indicate that fuzzy binding mode resemblance can be successfully exploited in docking screens, even in instances in which no crystallographic information is available, and suggest the use of pose ensembles for compound selection from GPCR homology models as an alternative to scoring.

AUTHOR INFORMATION

Corresponding Author

*E-mail: bajorath@bit.uni-bonn.de. Phone: 49-228-2699-306.

ORCID

Jürgen Bajorath: 0000-0002-0557-5714

Author Contributions

The study was carried out and the manuscript written with contributions of all authors. All authors have approved the final version of the manuscript.

Notes

The authors declare no competing financial interest.

ACKNOWLEDGMENTS

We thank the OpenEye Scientific Software, Inc., for providing a free academic license of the OpenEye toolkit and Chemical Computing Group, Inc., for academic teaching licenses of the Molecular operating Environment.

REFERENCES

(1) Irwin, J. J.; Shoichet, B. K. Docking Screens for Novel Ligands Conferring New Biology. *J. Med. Chem.* **2016**, *59*, 4103−4120.

(2) Lavecchia, A.; Di Giovanni, C. Virtual Screening Strategies in Drug Discovery: A Critical Review. *Curr. Med. Chem.* **2013**, *20*, 2839−2860.

(3) Kairys, V.; Fernandes, M. X.; Gilson, M. Screening Drug-Like Compounds by Docking to Homology Models: a systematic Study. *J. Chem. Inf. Model.* **2006**, *46*, 365−379.

(4) Ferrara, P.; Jacoby, E. Evaluation of the Utility of Homology Models in High Throughput Docking. *J. Mol. Model.* **2007**, *13*, 897−905.

(5) Fan, H.; Irwin, J. J.; Webb, B. M.; Klebe, G.; Shoichet, B. K.; Sali, A. Molecular Docking Screens Using Comparative Models of Proteins. *J. Chem. Inf. Model.* **2009**, *49*, 2512−2527.

(6) Kobilka, B. K. G. Protein Coupled Receptor Structure and Activation. *Biochim. Biophys. Acta, Biomembr.* **2007**, *1768*, 794−807.

(7) Kobilka, B. K.; Schertler, G. F. X. New G-Protein-Coupled Receptor Crystal Structures: Insights and Limitations. *Trends Pharmacol. Sci.* **2008**, *29*, 79−83.

(8) Rosenbaum, D. M.; Rasmussen, S. G.; Kobilka, B. K. The Structure and Function of G-Protein-Coupled Receptors. *Nature* **2009**, *459*, 356−363.

(9) Tautermann, C. S. GPCR Structures in Drug Design, Emerging Opportunities with New Structures. *Bioorg. Med. Chem. Lett.* **2014**, *24*, 4073−4079.

(10) Weil, T.; Renner, S. Homology Model-Based Virtual Screening for GPCR Ligands Using Docking and Target-Biased Scoring. *J. Chem. Inf. Model.* **2008**, *48*, 1104−1117.

(11) Shoichet, B. K.; Kobilka, B. K. Structure-Based Drug Screening for G-Protein-Coupled Receptors. *Trends Pharmacol. Sci.* **2012**, *33*, 268−272.

(12) Carlsson, J.; Coleman, R. G.; Setola, V.; Irwin, J. J.; Fan, H.; Schlessinger, A.; Sali, A.; Roth, B. L.; Shoichet, B. K. Ligand Discovery from a Dopamine D3 Receptor Homology Model and Crystal Structure. *Nat. Chem. Biol.* **2011**, *7*, 769−778.

(13) Becker, O. M.; Shacham, S.; Marantz, Y.; Noiman, S. Modeling the 3D Structure of GPCRs: Advances and Application to Drug Discovery. *Curr. Opin. Drug Discovery Dev.* **2003**, *6*, 353−361.

(14) Costanzi, S. On the Applicability of GPCR Homology Models to Computer-Aided Drug Discovery: A Comparison between in Silico and Crystal structures of the β_2-Adrenergic Receptor. *J. Med. Chem.* **2008**, *51*, 2907−2914.

(15) Kitchen, D. B.; Decornez, H.; Furr, J. R.; Bajorath, J. Docking and Scoring in Virtual Screening for Drug Discovery: Methods and Applications. *Nat. Rev. Drug Discovery* **2004**, *3*, 935−949.

(16) Moitessier, N.; Englebienne, P.; Lee, D.; Lawandi, J.; Corbeil, A. C. Towards the Development of Universal, Fast and Highly Accurate Docking/Scoring Methods: A Long Way to Go. *Br. J. Pharmacol.* **2008**, *153*, S7−S26.

(17) Huang, S.-Y.; Grinter, S. Z.; Zou, X. Scoring Functions and Their Evaluation Methods for Protein−ligand Docking: Recent Advances and Future Directions. *Phys. Chem. Chem. Phys.* **2010**, *12*, 12899−12908.

(18) Wang, J. C.; Lin, J. H. Scoring Functions for Prediction of Protein-Ligand Interactions. *Curr. Pharm. Des.* **2013**, *19*, 2174−2182.

(19) Cleves, A. E.; Jain, A. N. Knowledge-Guided Docking: Accurate Prospective Prediction of Bound Configurations of Novel Ligands Using Surflex-Dock. *J. Comput-Aided Mol. Des.* **2015**, *29*, 485−509.

(20) Kooistra, A. J.; Vischer, H. F.; McNaught-Flores, D.; Leurs, R.; De Esch, I. J.; De Graaf, C. Function-Specific Virtual Screening for GPCR Ligands Using a Combined Scoring Method. *Sci. Rep.* **2016**, *6*, No. 28288.

(21) Drwal, M. N.; Griffith, R. Combination of Ligand- and Structure-Based Methods in Virtual Screening. *Drug Discovery Today: Technol.* **2013**, *10*, No. e395.

(22) Broccatelli, F.; Brown, N. Best of Both Worlds: On the Complementarity of Ligand-Based and Structure-Based Virtual Screening. *J. Chem. Inf. Model.* **2014**, *54*, 1634−1641.

(23) Maggiora, G.; Vogt, M.; Stumpfe, D.; Bajorath, J. Molecular Similarity in Medicinal Chemistry. *J. Med. Chem.* **2014**, *57*, 3186−3204.

(24) Chen, Z.; Tian, G.; Wang, Z.; Jiang, H.; Shen, J.; Zhu, W. Multiple Pharmacophore Models Combined with Molecular Docking: A Reliable Way for Efficiently Identifying Novel PDE4 Inhibitors with High Structural Diversity. *J. Chem. Inf. Model.* **2010**, *50*, 615−625.

(25) Pappalardo, M.; Shachaf, N.; Basile, L.; Milardi, D.; Zeidan, M.; Raiyn, J.; Guccione, S.; Rayan, A. Sequential Application of Ligand and Structure Based Modeling Approaches to Index Chemicals for Their hH4R Antagonism. *PLoS One* **2014**, *9*, No. e109340.

(26) Sastry, G. M.; Inakollu, V. S. S.; Sherman, W. Boosting Virtual Screening Enrichments with Data Fusion: Coalescing Hits from Two-Dimensional Fingerprints, Shape, and Docking. *J. Chem. Inf. Model.* **2013**, *53*, 1531−1542.

(27) Anighoro, A.; Bajorath, J. Three-Dimensional Similarity in Molecular Docking: Prioritizing Ligand Poses on the Basis of Experimental Binding Modes. *J. Chem. Inf. Model.* **2016**, *56*, 580−587.

(28) Anighoro, A.; Bajorath, J. Binding Mode Similarity Measures for Ranking of Docking Poses: A Case Study on the Adenosine A_{2A} Receptor. *J. Comput-Aided Mol. Des.* **2016**, *30*, 447−456.

(29) Bajorath, J. Pushing the Boundaries of Computational Approaches: Special Focus Issue on Computational Chemistry and Computer-Aided Drug Discovery. *Future Med. Chem.* **2015**, *7*, 2415−2417.

(30) Cherezov, V.; Rosenbaum, D. M.; Hanson, M. A.; Rasmussen, S. G. F.; Thian, F. S.; Kobilka, T. S.; Choi, H.-J.; Kuhn, P.; Weis, W. I.; Kobilka, B. K.; Stevens, R. C. High-Resolution Crystal Structure of an Engineered Human beta2-Adrenergic G Protein-Coupled Receptor. *Science* **2007**, *318*, 1258−1265.

DOI: 10.1021/acsomega.7b00330
ACS Omega 2017, 2, 2583−2592

(31) *Molecular Operating Environment*, version 2014.09; Chemical Computing Group, Inc.
(32) Miller-Gallacher, J. L.; Nehmé, R.; Warne, T.; Edwards, P. C.; Schertler, G. F. X.; Leslie, A. G. W.; Tate, C. G. The 2.1 Å Resolution Structure of Cyanopindolol-Bound β_1-Adrenoceptor Identifies an Intramembrane Na+ Ion That Stabilises the Ligand-Free Receptor. *PLoS One* **2014**, *9*, No. e92727.
(33) Liu, W.; Chun, E.; Thompson, A. A.; Chubukov, P.; Xu, F.; Katritch, V.; Han, G. W.; Roth, C. B.; Heitman, L. H.; IJzerman, A. P.; Cherezov, V.; Stevens, R. C. Structural Basis for Allosteric Regulation of GPCRs by Sodium Ions. *Science* **2012**, *337*, 232−236.
(34) Sievers, F.; Wilm, A.; Dineen, D.; Gibson, T. J.; Karplus, K.; Li, W.; Lopez, R.; McWilliam, H.; Remmert, M.; Söding, J.; Thompson, J. D.; Higgins, D. G. Fast, Scalable Generation of High-Quality Protein Multiple Sequence Alignments Using Clustal Omega. *Mol. Syst. Biol.* **2011**, *7*, 539.
(35) Sali, A.; Blundell, T. L. Comparative Protein Modelling by Satisfaction of Spatial Restraints. *J. Mol. Biol.* **1993**, *234*, 779−815.
(36) Isberg, V.; Mordalski, S.; Munk, C.; Rataj, K.; Harpsøe, K.; Hauser, A. S.; Vroling, B.; Bojarski, A. J.; Vriend, G.; Gloriam, D. E. GPCRdb: An Information System for G Protein-Coupled Receptors. *Nucleic Acids Res.* **2016**, *44*, D356−D364.
(37) Kufareva, I.; Katritch, V.; et al. Participants of GPCR Dock 2013; Stevens, R. C.; Abagyan, R. Advances in GPCR Modeling Evaluated by the GPCR Dock 2013 Assessment: Meeting New Challenges. *Structure* **2014**, *22*, 1120−1139.
(38) Bauer, M. R.; Ibrahim, T. M.; Vogel, S. M.; Boeckler, F. M. Evaluation and Optimization of Virtual Screening Workflows with DEKOIS 2.0 − A Public Library of Challenging Docking Benchmark Sets. *J. Chem. Inf. Model.* **2013**, *53*, 1447−1462.
(39) Liu, T.; Lin, Y.; Wen, X.; Jorissen, R. N.; Gilson, M. K. BindingDB: A Web-Accessible Database of Experimentally Determined Protein−ligand Binding Affinities. *Nucleic Acids Res.* **2007**, *35*, D198−D201.
(40) Southan, C.; Sharman, J. L.; Benson, H. E.; Faccenda, E.; Pawson, A. J.; Alexander, S. P. H.; Buneman, O. P.; Davenport, A. P.; McGrath, J. C.; Peters, J. A.; Spedding, M.; Catterall, W. A.; Fabbro, D.; Davies, J. A. NC-IUPHAR. The IUPHAR/BPS Guide to PHARMACOLOGY in 2016: Towards Curated Quantitative Interactions between 1300 Protein Targets and 6000 Ligands. *Nucleic Acids Res.* **2016**, *44*, D1054−D1068.
(41) Mysinger, M. M.; Carchia, M.; Irwin, J. J.; Shoichet, B. K. Directory of Useful Decoys, Enhanced (DUD-E): Better Ligands and Decoys for Better Benchmarking. *J. Med. Chem.* **2012**, *55*, 6582−6594.
(42) Anighoro, A.; Rastelli, G. Enrichment Factor Analyses on G-Protein Coupled Receptors with Known Crystal Structure. *J. Chem. Inf. Model.* **2013**, *53*, 739−743.
(43) Peltason, L.; Bajorath, J. Molecular Similarity Analysis Uncovers Heterogeneous Structure-Activity Relationships and Variable Activity Landscapes. *Chem. Biol.* **2007**, *14*, 489−497.
(44) Willett, P.; Barnard, J. M.; Downs, G. M. Chemical Similarity Searching. *J. Chem. Inf. Model.* **1998**, *38*, 983−996.
(45) Bender, A.; Glen, R. C. A Discussion of Measures of Enrichment in Virtual Screening: Comparing the Information Content of Descriptors with Increasing Levels of Sophistication. *J. Chem. Inf. Model.* **2005**, *45*, 1369−1375.
(46) Lätti, S.; Niinivehmas, S.; Pentikäinen, O. T. Rocker: Open Source, Easy-to-use Tool for AUC and Enrichment Calculations and ROC Visualization. *J. Cheminform.* **2016**, *8*, 45.
(47) Truchon, J.-F.; Bayly, C. I. Evaluating Virtual Screening Methods: Good and Bad Metrics for the "Early Recognition" Problem. *J. Chem. Inf. Model.* **2007**, *47*, 488−508.
(48) Ramírez, M. J. 5-HT$_6$ Receptors and Alzheimer's Disease. *Alzheimer's Res. Ther.* **2013**, *5*, 15.
(49) Karila, D.; Freret, T.; Bouet, V.; Boulouard, M.; Dallemagne, P.; Rochais, C. Therapeutic Potential of 5-HT$_6$ Receptor Agonists. *J. Med. Chem.* **2015**, *58*, 7901−7912.
(50) Wang, C.; Jiang, Y.; Ma, J.; Wu, H.; Wacker, D.; Katritch, V.; Han, G. W.; Liu, W.; Huang, X.-P.; Vardy, E.; McCorvy, J. D.; Gao, X.; Zhou, X. E.; Melcher, K.; Zhang, C.; Bai, F.; Yang, H.; Yang, L.; Jiang, H.; Roth, B. L.; Cherezov, V.; Stevens, R. C.; Xu, H. E. Structural Basis for Molecular Recognition at Serotonin Receptors. *Science* **2013**, *340*, 610−614.
(51) Liu, W.; Wacker, D.; Gati, C.; Han, G. W.; James, D.; Wang, D.; Nelson, G.; Weierstall, U.; Katritch, V.; Barty, A.; Zatsepin, N. A.; Li, D.; Messerschmidt, M.; Boutet, S.; Williams, G. J.; Koglin, J. E.; Seibert, M. M.; Wang, C.; Shah, S. T. A.; Basu, S.; Fromme, R.; Kupitz, C.; Rendek, K. N.; Grotjohann, I.; Fromme, P.; Kirian, R. A.; Beyerlein, K. R.; White, T. A.; Chapman, H. N.; Caffrey, M.; Spence, J. C. H.; Stevens, R. C.; Cherezov, V. Serial Femtosecond Crystallography of G Protein-Coupled Receptors. *Science* **2013**, *342*, 1521−1524.
(52) Sleight, A. J.; Boess, F. G.; Bös, M.; Levet-Trafit, B.; Riemer, C.; Bourson, A. Characterization of Ro 04-6790 and Ro 63-0563: Potent and Selective Antagonists at Human and Rat 5-HT6 Receptors. *Br. J. Pharmacol.* **1998**, *124*, 556−562.

DOI: 10.1021/acsomega.7b00330
ACS Omega 2017, 2, 2583−2592